

## Electropolymerization of Bis(2-cyano-2- $\alpha$ -thienylethenyl)arylenes

Shi-Chun Lin, Jau-An Chen, Mao-Huang Liu, Y. Oliver Su,\* and Man-kit Leung\*

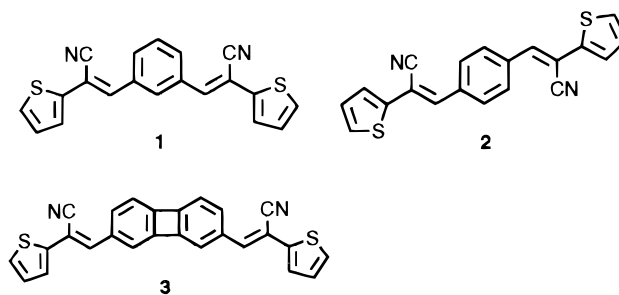
Department of Chemistry, National Taiwan University, Taipei, Taiwan, Republic of China

Received February 9, 1998

The synthesis and the electrochemical studies of 1,3-bis(2-cyano-2- $\alpha$ -thienylethenyl)benzene (**1**), 1,4-bis(2-cyano-2- $\alpha$ -thienylethenyl)benzene (**2**), and 2,7-bis(2-cyano-2- $\alpha$ -thienylethenyl)biphenylene (**3**) are reported herein. While compound **2** could be reversibly reduced to form the corresponding dianion, compounds **1** and **3** show irreversible or quasireversible reductions in their cyclic voltammetric studies. We tentatively attribute the high reactivity of the dianions of **1** and **3** to their diradicaloid behavior. This explanation is further supported by PM3/RHF–PM3/UHF calculations. Compounds **1–3** could be irreversibly oxidized at the potential more positive than +1.3 V. Among these compounds, **3** shows the highest reactivity toward oxidative electropolymerization. The resulting polymer film is relatively stable and electroactive. Although polymeric films of compounds **1** and **2** could be formed at higher monomer concentrations, the films are unstable toward electrochemical oxidation. UV–vis analyses of the polymeric films reveal that electropolymerization of **2** is quenched at the early stage of the polymerization, resulting in significant amounts of oligomers in the matrix. However, biphenylene containing monomer **3** could be smoothly converted to highly conjugated polymers under electrochemical oxidation.

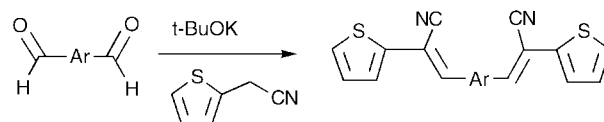
Because of their intriguing physicochemical properties as well as practical applications, conjugated polymers have attracted considerable attention during the last few decades. Most of the conjugated polymers that have been studied are containing aromatic  $6\pi$ -electron units as the fundamental building blocks.<sup>1–9</sup> In addition, many other conjugated oligomers or polymers containing aromatic ( $4n + 2$ )  $\pi$ -electron systems, such as naphthalene, anthracene, and fused-ring heterocycles, have also been investigated. However, conjugated polymers based on ( $4n$ )  $\pi$ -electron systems are surprisingly rare.<sup>3,10</sup> To exploit the potential of applying the unusual electrochemical properties of antiaromatic ( $4n$ )  $\pi$ -electron units to conjugated polymer systems, we have recently focused our research on novel polymers that contain biphenylene or its derivatives as the building blocks. Our previous investigation revealed that oligo(2,7-biphenylene)-(*E*-

vinylene)s can be either oxidized or reduced electrochemically.<sup>11</sup> These observations prompted us to further study the redox behavior of related polymers. To avoid problematic coating processes due to the low solubility of conjugated polymers, we decide to electrogenerate polymeric thin films directly on electrode surfaces. We herein report the syntheses and the studies of the electrochemical behavior of **1–3**. The object of the investigation is to explore the effects arising from an antiaromatic biphenylene unit on electropolymerization.



### Results and Discussion

The syntheses of monomers **1–3** were accomplished by employing the Knoevenagel-type coupling of dialdehydes **4–6** with 2-(cyanomethyl)thiophene under basic conditions. While isophthalaldehyde (**4**) and terephthalaldehyde



**4** Ar = *m*-C<sub>6</sub>H<sub>4</sub>

**5** Ar = *p*-C<sub>6</sub>H<sub>4</sub>

**6** Ar = 2,7-biphenylene

**1** Ar = *m*-C<sub>6</sub>H<sub>4</sub>

**2** Ar = *p*-C<sub>6</sub>H<sub>4</sub>

**3** Ar = 2,7-biphenylene

(**5**) are commercially available, dialdehyde **6** was synthesized from diester **7** through a two-step synthetic sequence of LiAlH<sub>4</sub> reduction and PCC oxidation. The

\* To whom correspondence should be addressed. Tel.: +886 2 23690152 ext 121. Fax: +886 2 23636359. E-mail: mkleung@ms.cc.ntu.edu.tw.

(1) For general reviews, see: (a) Seanor, D. A. *Electrical Properties of Polymers*; Academic Press: New York, 1982. (b) Skotheim, T. A. *Handbook of Conducting Polymers, Vol. 1 and 2*; Marcel Dekker: New York, 1986. (c) Ku, C. C.; Liepins, R. *Electrical Properties of Polymers-Chemical Principles*; Hanser Publisher: New York, 1987. (d) Aldissi, M. *Inherently Conducting Polymers. Processing, Fabrication, Applications, Limitations*; Noyes Data Corp.: 1989. (e) Brédas, J. L.; Silbey, R. *Conjugated Polymers. The Novel Science and Technology of Highly Conducting and Nonlinear Optically Active Materials*; Kluwer Academic Publishers: Dordrecht, 1991.

(2) Kovacic, P.; Jones, M. B. *Chem. Rev.* **1987**, *87*, 357.

(3) Scherf, U.; Müllen, K. *Synthesis* **1992**, 23.

(4) Burn, P. L.; Holmes, A. B.; Kraft, A.; Bradley, D. D. C.; Brown, A. R.; Friend, R. H.; Gymer, R. W. *Nature* **1992**, *356*, 47.

(5) Bäuerle, P. *Adv. Mater.* **1993**, *5*, 879.

(6) (a) Miller, J. S. *Adv. Mater.* **1993**, *5*, 578. (b) Miller, J. S. *Adv. Mater.* **1990**, *2*, 98.

(7) Mark, T. J.; Ratner, M. A. *Angew. Chem., Int. Ed. Engl.* **1995**, *34*, 155.

(8) Giesa, R. *J. Macromol. Sci.; Rev. Macromol. Chem. Phys.* **1996**, *C36(4)*, 631.

(9) (a) Roncali, J. *Chem. Rev.* **1997**, *97*, 173. (b) Roncali, J. *Chem. Rev.* **1992**, *92*, 771.

(10) Aughter-Krummel, P.; Müllen, K. *Angew. Chem., Int. Ed. Engl.* **1991**, *30*, 1003.

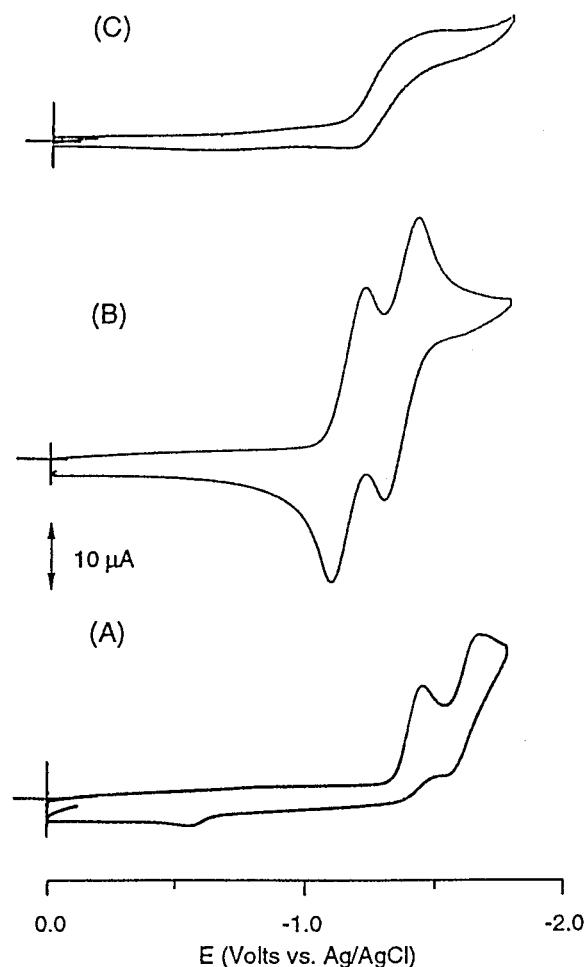


**Figure 1.** Reductive cyclic voltammograms of **1–3** in 0.1 M  $\text{Bu}_4\text{NClO}_4\text{-CH}_2\text{Cl}_2$ , scan rate  $100\text{ mV s}^{-1}$ : (A) voltammogram of **1**; (B) voltammogram of **2**; (C) voltammogram of **3**.

details of the preparation of dialdehyde **6** have been reported in our recent publications.<sup>11</sup>

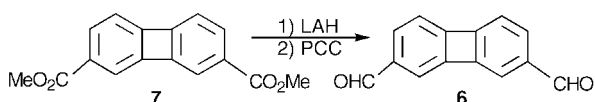
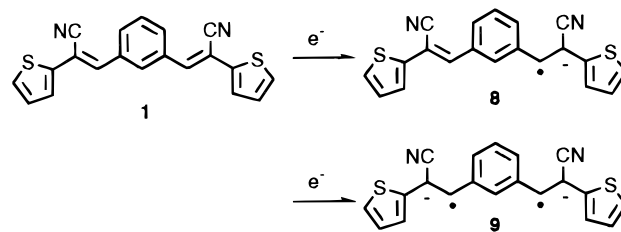


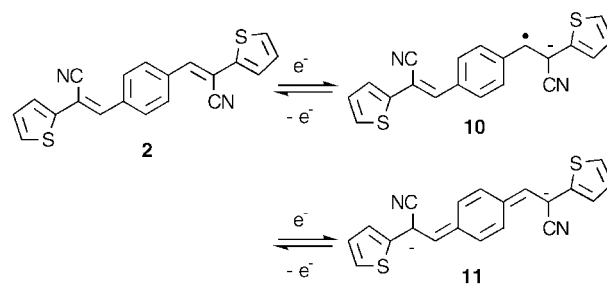
Figure 1A–C illustrates the reductive cyclic voltammograms of **1–3**. The voltammogram of **1** (Figure 1A) shows two reduction waves in which the first wave is irreversible at  $E_p = -1.44\text{ V}$  while the second reduction is quasireversible at  $E_{1/2} = -1.60\text{ V}$ . The reduction behavior of **1** could be explained in terms of the formation of **9**, an open-shell dianion–diradical through sequential one-electron reductions (Scheme 1). Due to the high reactivity of **8** and **9**, both intermediates are labile, resulting in the quasireversible and irreversible waves in the cyclic voltammogram.

Unlike the meta analogue, monomer **2** transforms reversibly to the closed-shell dianion **11** through two successive reductions (Figure 1B).<sup>12</sup> The formal potentials ( $E_{1/2}$ ) are  $-1.14$  and  $-1.34\text{ V}$ , respectively. The reversible waves in the cyclic voltammogram could

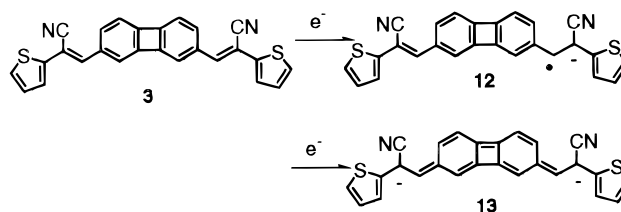
**Scheme 1**



be attributed to the relatively high stability of **10** and **11**. Since dianion **11** possesses a closed-shell singlet ground state, higher stability of **11** in comparison to the open-shell dianion–diradical **9** is to be expected. In addition, stabilization of anion–radical **10** through conjugation with the para substituent is also anticipated.



In contrast, biphenylene derivative **3** exhibits an irreversible reduction starting at  $-1.12\text{ V}$  (Figure 1C). The broad wave in the reductive scan suggests the exist of two successive reduction waves closely spaced with each other. The first reduction peak-potential appearing in the vicinity of  $-1.25\text{ V}$  is apparently lower than that of **1** but close to that of **2**, suggesting the presence of a low-lying LUMO arising from conjugation between two electron-withdrawing cyano substituents. The small difference between the first and the second reduction potentials indicates a small Coulombic repulsion between the negative charges on the molecule. Although the Kekulé valence structure of the dianion suggests a singlet ground state for **13**, the closed-shell valence assignment could not clearly explain the unexpectedly high reactivity.

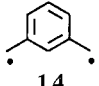
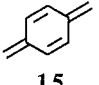
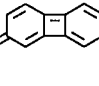


To obtain an insight into the origin of the reactivity, we carried out PM3/RHF and PM3/UHF computations for the heats of formation of the lowest singlet states and triplet states of **14–16**, and their energy differences ( $\Delta E_{T-S}^{\text{calcd}}$ ) were calculated (Table 1). To test the reliability of this computational approach, correlation of the calculated  $\Delta E_{T-S}^{\text{calcd}}$  with the experimental  $\Delta E_{T-S}^{\text{exptl}}$  for

(11) (a) Kwong, C.-Y.; Chan, T.-L.; Chow, H.-F.; Lin, S.-C.; Leung, M.-k. *J. Chin. Chem. Soc.* **1997**, *44*, 211. (b) Kwong, C.-Y.; Leung, M.-k.; Lin, S.-C.; Chan, T.-L.; Chow, H.-F. *Tetrahedron Lett.* **1996**, *37*, 5913.

(12) Similar reversible reduction behavior for the 2,5-substituted thiophene analogue has recently been reported. For reference, see: Ho, H. A.; Brisset, H.; Elandaloussi, E.; Frère, P.; Roncali, J. *Adv. Mater.* **1996**, *8*, 990.

**Table 1.** Calculated and Estimated Values of  $\Delta E_{(T-S)}$  for 14–16

Compound	calculated	Estimated <sup>a</sup>
	$\Delta E_{(T-S)}$ (eV)	$\Delta E_{(T-S)}$ (eV)
	-0.58	-0.013
	0.38	1.2
	-0.67	-0.11

<sup>a</sup> The values were estimated according to the empirical equation ( $\Delta E_{(T-S)}^{\text{estd}} = 16.2 + 1.23 (\Delta E_{(T-S)}^{\text{calcd}}$ ) derived from the correlation plot in Figure 2.

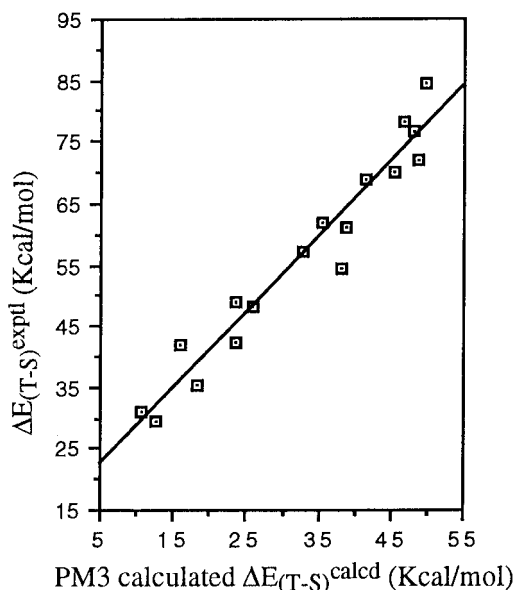
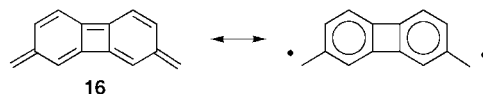


**Figure 2.** Comparison of PM3 calculated and experimental values of  $\Delta E_{(T-S)}$ . The plot shows a linear correlation of  $\Delta E_{(T-S)}^{\text{exptl}} = 16.2 + 1.23\Delta E_{(T-S)}^{\text{calcd}}$  with the correlation coefficient  $r = 0.96$ .

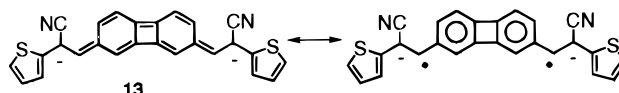
17 known aromatic compounds was examined.<sup>13</sup> The correlation plot (Figure 2) shows that the calculated values are linearly correlated to the experimental data with  $r = 0.96$ . The empirical expression of correlation equation is  $\Delta E_{T-S}^{\text{exptl}} = 16.2 + 1.23\Delta E_{T-S}^{\text{calcd}}$ . The estimated energy differences for the triplet and singlet states ( $\Delta E_{T-S}$ ) of 14–16 were then determined from the corresponding values of  $\Delta E_{T-S}^{\text{calcd}}$  listed in Table 1 as well as the empirical correlation equation derived from Figure 2. To our surprise, the results of the PM3 calculations indicate that the lowest triplet state of 16 is slightly preferable than, or almost degenerated from, the corre-

(13) The 17 known aromatic compounds used in the correlation plot are benzene, anthracene, naphthalene, benzonitrile, benzaldehyde, 1,4-dicyanobenzene, azulene, *trans*-stilbene, pyrene, perylene, ethylene, tetracene, benzo(3,4)pyrene, fluorene, phenanthrene, chrysenes, and coronene. Computations were performed using Hyperchem version 4. The experimental values of  $\Delta E_{T-S}^{\text{exptl}}$  for the 17 known aromatic compounds were obtained from: Murov, M. L. *Handbook of Photochemistry*; Marcel Dekker: New York, 1973.

sponding singlet state. This finding is contrast to the Kekulé valence prediction, implying a strong diradical character of 16. We tentatively rationalized this result in terms of restoration of aromaticity in the diradical form of 16, which makes the triplet state preferable than the corresponding singlet state. On the basis of the

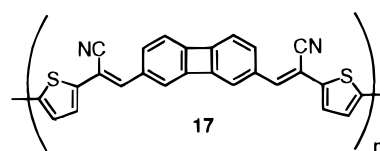


calculations, one may reasonably attribute the irreversible reduction behavior of 13 to its highly reactive diradical or diradicaloid ground-state character.



Nevertheless, the possibility of reductive ring-opening of the central biphenylene unit could not be eliminated. It has been reported that the biphenylene dianion is unstable above 0 °C, giving the dilithiobiphenyl as the final product.<sup>14</sup>

Monomers 1–3 can be irreversibly oxidized at the potential more positive than +1.3 V. Among these compounds, 3 shows the highest reactivity toward electropolymerization. Figure 3A shows the repeated CV of 3 at the concentration of 0.001 M, utilizing Pt as the working electrode. The first CV trace shows an irreversible anodic wave corresponding to the oxidation of 3 into its cation-radical. Subsequent cycling leads to the emergence of a new redox system at less positive potential. Deposition of a purple polymeric film on the electrode surface in the successive cycles can be clearly observed. After 25 cycles, the polymer film of 17 was rinsed with  $\text{CH}_2\text{Cl}_2$  and moved to a monomer-free supporting electrolyte solution. Cyclic voltammetric analysis of the



polymer shows reversibly redox cycles with oxidative and reductive peaks at +1.10 and +0.80 V, respectively (Figure 3B). Similar to monomer 3, the electrogenerated polymeric thin film of 17 is unstable toward electrochemical reduction. Although the film shows a reductive peak current at  $E_{\text{pc}} = -1.62$  V with the corresponding oxidative peak at -1.30 V at the first scan, the cyclic voltammogram becomes featureless upon reductive cycling.

Electropolymerizations of 1 and 2 are apparently less effective at low monomer concentrations. However, film

(14) Benken, R.; Finneiser, K.; von Puttkamer, H.; Günther, H.; Eliasson, B.; Edlund, U. *Helv. Chim. Acta* **1986**, *69*, 955.15. For general reviews of biphenylene chemistry, see: (a) Barton, J. W. *Nonbenzenoid Aromatics*; Academic Press: New York, 1969; Vol. 1, p 32. (b) Lloyd, D. *Nonbenzenoid Conjugated Carbocyclic Compounds*; Elsevier: Amsterdam, 1984, p 216. (c) Vögtle, F. *Fascinating Molecules in Organic Chemistry*; Wiley: New York, 1992; p 111. (d) Snyder, J. P. *Nonbenzenoid Aromatics*; Academic Press: New York, 1969; Vol. 1. (e) Cava, M. P.; Mitchell, M. J. *Cyclobutadiene and Related Compounds*; Academic Press: New York, 1967. (f) Toda, F.; Garratt, P. *Chem. Rev.* **1992**, *92*, 1685.

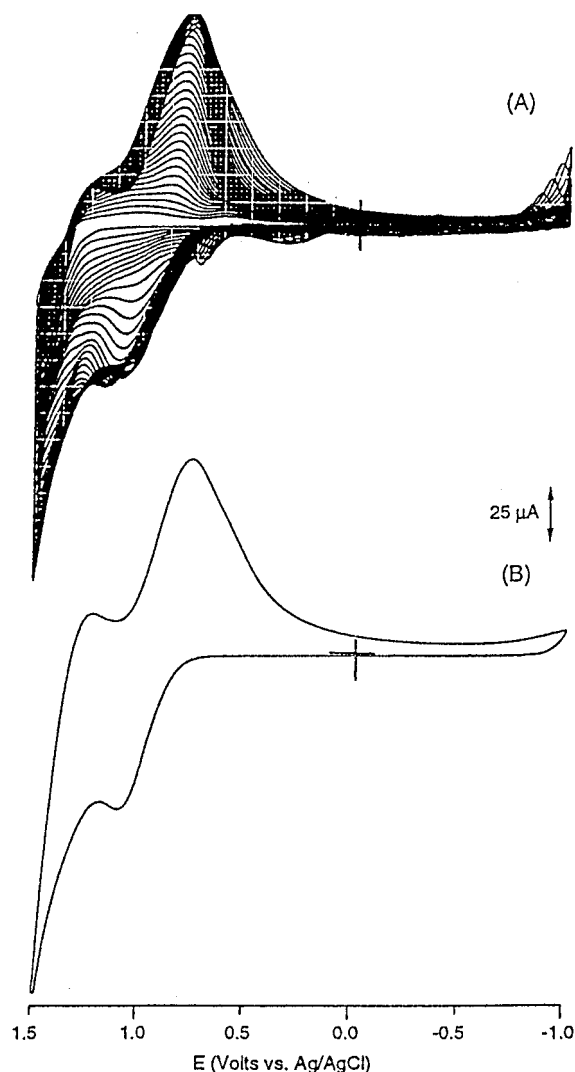


**Figure 3.** (A) Growth of a poly(2,7-bis[2-cyano-2- $\alpha$ -thienyl]ethenyl)biphenylene (**17**) film on a Pt electrode in 0.1 M  $\text{Bu}_4\text{NClO}_4\text{-CH}_2\text{Cl}_2$ , scan rate 100 mV; (B) cyclic voltammogram of **17** at a Pt electrode in a monomer-free supporting electrolyte solution (0.1 M  $\text{Bu}_4\text{NClO}_4\text{-CH}_2\text{Cl}_2$ ), scan rate 100 mV.

growth can be facilitated by increasing the monomer concentrations to 0.025 M. Unfortunately, as the "polythiophene paradox"<sup>9b</sup> predicted, these polymer films are unstable at the potentials required for their formation. Degradation of the polymer competes with its electrodeposition, inhibiting the film growth process after a few cycles, and the reversible redox features of the newly formed electroactive polymers gradually decay.

The above conclusions are further evidenced by UV-vis spectral analysis. Monomer **1** shows an absorption maximum ( $\lambda_{\text{max}}$ ) at 351 nm ( $\epsilon = 2.0 \times 10^4$ ). However, due to the effects of conjugation, monomer **2** has an absorption maximum shifted to 395 nm ( $\epsilon = 1.8 \times 10^4$ ). On the other hand, monomer **3** shows two absorption bands, which are characteristic for biphenylene and its derivatives,<sup>11,14</sup> with the maxima at 337 nm (band I,  $\epsilon = 4.1 \times 10^4$ ) and 465 nm (band II,  $\epsilon = 3.0 \times 10^4$ ), respectively.

Polymer films for spectral analysis were directly electrogenerated on ITO glass. Because of the nonconjugative properties of the *meta*-phenylene spacing unit, a thin film of **18** shows an absorption maximum at 360 nm

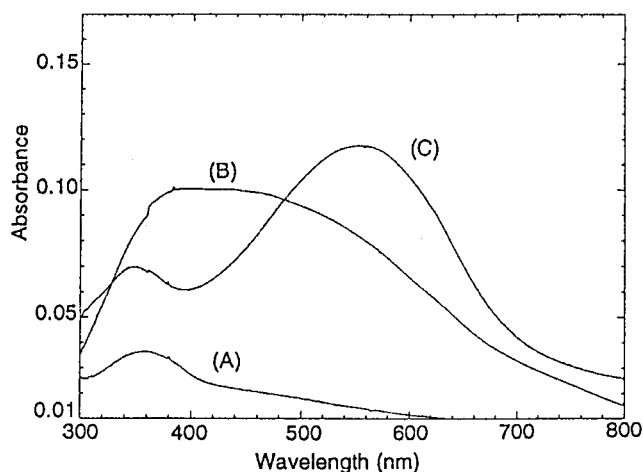
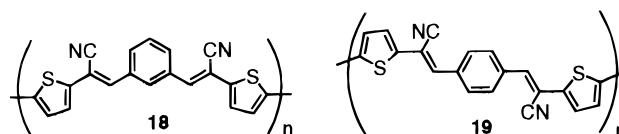


**Figure 4.** UV-vis spectra of electrogenerated **17–19** on ITO-coated glass: (A) absorption spectrum of **18**; (B) absorption spectrum of **19**; (C) absorption spectrum of **17**.

along with the band edge extended to 450 nm (Figure 4, spectrum A). On the other hand, electropolymerized **19**



has an extremely broad absorption band ranging from 300 to 700 nm (Figure 4, spectrum B). This observations are consistent with the results of the cyclic voltammetric analyses. The competitive degradation during electropolymerization inhibits the growth of the polymer chains, resulting conjugated polymers with a broad molecular-weight distribution. Since the oligomeric components absorb at shorter wavelength regions while the highly conjugated polymeric components absorb at longer wavelength regions, they constitute a thin film that has an extremely broad absorption region. In contrast, the spectrum of **17** (Figure 4, spectrum C) shows clearly two distinct absorption bands with the maxima centered at 350 nm (band I) and 560 nm (band II). Similar to our observations for other biphenylene systems, the absorption maximum of band I does not shift significantly in respect to the extent of conjugation, while the maximum of the band II shifts bathochromically to 560 nm (2.2 eV) with the band edge extended to 700 nm (1.7 eV).<sup>11</sup> In addition, the absorption intensity of band II relative to band I is apparently enhanced. The narrow and symmetrical shape of band II is in good agreement with the results of the cyclic voltammetric analysis, indicating that the film is constituted predominantly by highly conjugated polymeric components.

Our present results demonstrated the importance of the biphenylene unit in the oxidative electropolymerization. Previous work on oligo(2,7-biphenylenylene-(*E*)-vinylene)s indicated that biphenylene-containing conjugated molecules tend to delocalize positive charges over the conjugated  $\pi$ -systems.<sup>11,14</sup> Since typical mechanisms for electropolymerization of thiophenes involve coupling of the corresponding cation radicals, effective dispersion of the positive charge over the cation-radical of **3** may largely reduce the intermolecular electrostatic repulsion between the radical cations, increasing the tendency toward polymerization.

### Experimental Section

**A General Procedure for the Preparation of Monomers 1–3.** **1,3-Bis(2-cyano-2- $\alpha$ -thienylethenyl)benzene (1).** To a suspension of potassium *tert*-butoxide (2.8 g, 0.023 mol) in EtOH (50 mL) was added a solution of isophthalaldehyde (**4**) (1.5 g, 0.011 mol) and 2-(cyanomethyl)thiophene (2.8 g, 0.023 mol) in EtOH (10 mL) under an atmosphere of nitrogen. The mixture was allowed to react at room temperature for 3 h. The reaction was quenched by rotary evaporation of the EtOH followed by addition of water. The crude products were extracted with CH<sub>2</sub>Cl<sub>2</sub>, dried over anhydrous Mg<sub>2</sub>SO<sub>4</sub>, and purified by liquid chromatography on silica gel, using CH<sub>2</sub>Cl<sub>2</sub>–hexanes (1:1) as eluent to obtain **1** as a yellowish solid (3.1 g, 82%). Recrystallization of **1** from DMSO–EtOAc (2:1) provided yellowish crystals: mp 126–128 °C; <sup>1</sup>H NMR (300 MHz, CDCl<sub>3</sub>)  $\delta$  8.06 (s, 1H), 7.96 (d,  $J$  = 7.9 Hz, 2H), 7.54 (t,  $J$  = 7.9 Hz, 1H), 7.41 (d,  $J$  = 3.6 Hz, 2H), 7.32 (d,  $J$  = 5.0 Hz, 2H), 7.07 (dd,  $J_1$  = 3.6 Hz,  $J_2$  = 5.0 Hz, 2H); <sup>13</sup>C NMR (75 MHz, CDCl<sub>3</sub>)  $\delta$  138.75, 138.19, 134.71, 130.22, 130.10, 139.72, 128.18, 127.80, 126.75, 116.51, 107.49; UV–vis (CHCl<sub>3</sub>, 2.1  $\times$  10<sup>-5</sup> M)  $\lambda_{\max}$  351 nm ( $\epsilon$  = 20 761); MS  $m/z$  (EI, 70 eV) 344 (100), 316 (20), 283 (20), 259 (20), 209 (30); HRMS (M<sup>+</sup>) calcd for C<sub>20</sub>H<sub>12</sub>N<sub>2</sub>S<sub>2</sub> 344.0441, found 344.0449. Anal. Calcd for C<sub>20</sub>H<sub>12</sub>N<sub>2</sub>S<sub>2</sub>: C, 69.73; H, 3.52; N, 8.14. Found: C, 69.72; H, 3.54; N, 8.07.

**1,4-Bis(2-cyano-2- $\alpha$ -thienylethenyl)benzene (2).** Liquid chromatography on silica gel, using CH<sub>2</sub>Cl<sub>2</sub>–hexanes (1:1) as eluent, gave **2** as a solid (81%). Recrystallization of **2** from DMSO–ethyl acetate (2:1) provided reddish-yellow crystals: mp 218–220 °C; <sup>1</sup>H NMR (200 MHz, CDCl<sub>3</sub>)  $\delta$  7.92 (s, 4H), 7.42 (d,  $J$  = 3.6 Hz, 2H), 7.35 (s, 2H), 7.33 (d,  $J$  = 5.1 Hz, 2H), 7.08 (dd,  $J_1$  = 3.6 Hz,  $J_2$  = 5.0 Hz, 2H); <sup>13</sup>C NMR (100 MHz, CDCl<sub>3</sub>)  $\delta$  139.07, 137.82, 135.08, 129.56, 128.25, 127.83, 126.84, 116.57, 107.36; UV–vis (CDCl<sub>3</sub>, 2.0  $\times$  10<sup>-5</sup> M)  $\lambda_{\max}$  395 nm ( $\epsilon$  = 18 163); MS  $m/z$  (EI, 70 eV) 344 (100), 315 (10), 283 (10), 233 (10), 209 (20); HRMS (M<sup>+</sup>) calcd for C<sub>20</sub>H<sub>12</sub>N<sub>2</sub>S<sub>2</sub> 344.0441, found 344.0452. Anal. Calcd for C<sub>20</sub>H<sub>12</sub>N<sub>2</sub>S<sub>2</sub>: C, 69.73; H, 3.52; N, 8.14. Found: C, 69.57; H, 3.60; N, 8.07.

**2,7-Bis(2-cyano-2- $\alpha$ -thienylethenyl)biphenylene (3).** Liquid chromatography on silica gel, using CH<sub>2</sub>Cl<sub>2</sub>–hexanes (1:1) as eluent, gave **3** as a solid (84%). Recrystallization of **3** from DMSO–EtOAc (2:1) provided reddish crystals: mp 221–223 °C; <sup>1</sup>H NMR (200 MHz, CDCl<sub>3</sub>)  $\delta$  7.39 (s, 2H), 7.35 (d,  $J$  =

3.6 Hz, 2H), 7.29 (d,  $J$  = 5.1 Hz, 2H), 7.22 (d,  $J$  = 7.8 Hz, 2H), 7.14 (s, 2H), 7.05 (dd,  $J_1$  = 3.6 Hz,  $J_2$  = 5.1 Hz, 2H), 6.79 (d,  $J$  = 7.8 Hz, 2H); <sup>13</sup>C NMR (100 MHz, CDCl<sub>3</sub>)  $\delta$  152.44, 151.00, 139.41, 139.22, 134.78, 132.58, 128.17, 127.28, 126.27, 118.44, 116.99, 116.82, 105.25; UV–vis (CDCl<sub>3</sub>, 1.96  $\times$  10<sup>-5</sup> M)  $\lambda_{\max}$  465 nm ( $\epsilon$  = 30 408), 337 nm ( $\epsilon$  = 41 173), 246 nm ( $\epsilon$  = 18 622); MS  $m/z$  (EI, 70 eV) 418 (100), 389 (10), 357 (10), 312 (10), 312 (20), 283 (20); HRMS (M<sup>+</sup>) calcd for C<sub>26</sub>H<sub>14</sub>N<sub>2</sub>S<sub>2</sub>: 418.0598, found 418.0603. Anal. Calcd for C<sub>26</sub>H<sub>14</sub>N<sub>2</sub>S<sub>2</sub>: C, 74.63; H, 3.38; N, 6.70. Found: C, 74.58; H, 3.52; N, 6.66.

**Cyclic Voltammetric Experiments for Monomers 1–3.** Tetrabutylammonium perchlorate (TBAP), the supporting electrolyte, was recrystallized twice from ethyl acetate before use. Dichloromethane, the solvent for electrochemical study, was distilled from CaH<sub>2</sub> and deaerated by purging with highly pure N<sub>2</sub> gas.

Cyclic voltammetry (CV) was conducted with an EG&G Princeton Applied Research Model 174A polarographic analyzer, EG&G PARC Model 175 universal programmer, and a BAS X-Y recorder. In a three-electrode cell, the working electrode was a glassy carbon disk with 0.07 cm<sup>2</sup> area. A platinum wire (0.25 mm in diameter) was used as an auxiliary electrode. A homemade Ag/AgCl reference electrode was used and was calibrated with a saturated calomel electrode. The error is within  $\pm$ 3 mV. All the potentials are reported relative to this reference. The formal potential of ferrocene in the electrochemical system is +0.525 V. The glassy carbon electrode was polished on a felt pad (Buehler) with alumina (0.5  $\mu$ m) to obtain a mirrorlike surface and then was placed in an ultrasonicator drum for 1 min to remove the residual alumina.

**Acknowledgment.** We thank the National Science Council of the Republic of China (NSC-87-2113-M-002-009) for financial support.

**Supporting Information Available:** <sup>1</sup>H NMR spectra of **1–3** (3 pages). This material is contained in libraries on microfiche, immediately follows this article in the microfilm version of the journal, and can be ordered from the ACS; see any current masthead page for ordering information.

JO980239M